

Review

The Emerging Career of Strontium Titanates in Photocatalytic Applications: A Review

Nikita Sharma ^{1,*}  and Klara Hernadi ^{2,*} 

¹ Advanced Materials and Intelligent Technologies Higher Education and Industrial Cooperation Centre, University of Miskolc, H-3515 Miskolc, Hungary

² Institute of Physical Metallurgy, Metal Forming and Nanotechnology, University of Miskolc, Miskolc-Egyetemváros, C/1 108, H-3515 Miskolc, Hungary

* Correspondence: nikita_sh18@yahoo.co.in (N.S.); klara.hernadi@uni-miskolc.hu (K.H.); Tel.: +36-46-565-111/1339 (N.S. & K.H.)

Abstract: The growing energy demands and rapid industrialization drove the attention towards a sustainable living. The methods to adopt renewable source of energy has made the field of heterogeneous photocatalysis so famous. The photocatalytic hydrogen production seems to be an answer for our future energy crisis. In this regard, alkaline earth metal titanates with a perovskite structure are one of the in demand materials these days. Among these, strontium titanates (SrTiO₃) play an important role and have shown a potential, especially in the field of hydrogen production. This review summarizes the significance of (SrTiO₃) in photocatalytic water splitting, to produce hydrogen and the photocatalytic degradation of the pollutants from the waste water. Different synthesis methods used for preparing SrTiO₃ are also discussed.

Keywords: hydrogen production; photodegradation; strontium titanate; titanates



Citation: Sharma, N.; Hernadi, K. The Emerging Career of Strontium Titanates in Photocatalytic Applications: A Review. *Catalysts* **2022**, *12*, 1619. <https://doi.org/10.3390/catal12121619>

Academic Editors: Roberto Fiorenza and Gilles Berhault

Received: 30 September 2022

Accepted: 6 December 2022

Published: 9 December 2022

Publisher's Note: MDPI stays neutral with regard to jurisdictional claims in published maps and institutional affiliations.



Copyright: © 2022 by the authors. Licensee MDPI, Basel, Switzerland. This article is an open access article distributed under the terms and conditions of the Creative Commons Attribution (CC BY) license (<https://creativecommons.org/licenses/by/4.0/>).

1. Introduction

The total dependence on the non-renewable energy sources has led humankind into a severe critical situation. Across the globe, the demand for fossil fuels is increasing tremendously with the constant growth in population. The unequal distribution of such resources, such as crude oil, across the planet is leading to overexploitation, which is creating an imbalance between the different nations, drastically affecting human life. The limited availability is not just the only problem, but the polluting of the most essential resources (water, air and soil) is posing a danger to the existence of the human era. The impact is such that the threat to clean food and water, extreme weather changes and the outbreak of life-threatening diseases, can be seen. Currently, two thirds of the global carbon emissions come from the energy sector. The subsidies supporting fossil fuels are over USD \$180 billion, while that for renewables is around half. Moreover, the promising results arising from the abundant renewable resources has helped scientists to spread the word. As a result, several agreements concerning renewables are being signed and are no longer planned within 50 years but within 5 years.

Solar is the most abundant renewable energy source and by far has the potential to be efficiently harnessed. According to Key World Energy Statistics 2020, around 35% of energy consumption is in the transport sector, as shown in Figure 1. This shows a huge dependence of our current infrastructure on liquid fuels. In order to reverse this dependency towards the renewable side, many studies have been carried out, to produce “greener” fuels, meaning with low or no carbon emissions. This is where the concept of hydrogen fuel comes from. Recently, the growing number of reports has been focusing on generating hydrogen fuels with the use of solar energy. At present, more than 90% of hydrogen is produced by an energy-intensive method of the steam reforming of fossil fuels, which generates CO₂, thereby, increasing the greenhouse gas emissions which are

responsible for global warming. One of the feasible ways to produce hydrogen is by a solar thermochemical way, which can be more energy efficient, compared to the conventional method. In this way, a sustainable route of hydrogen production could be developed, since it leads to zero carbon emissions. However, its production is a challenging task. The efficiencies reported so far are too low for implementing in the real world. Therefore, much work is still required, to develop/design materials that can make efficient use of energy from the sun.

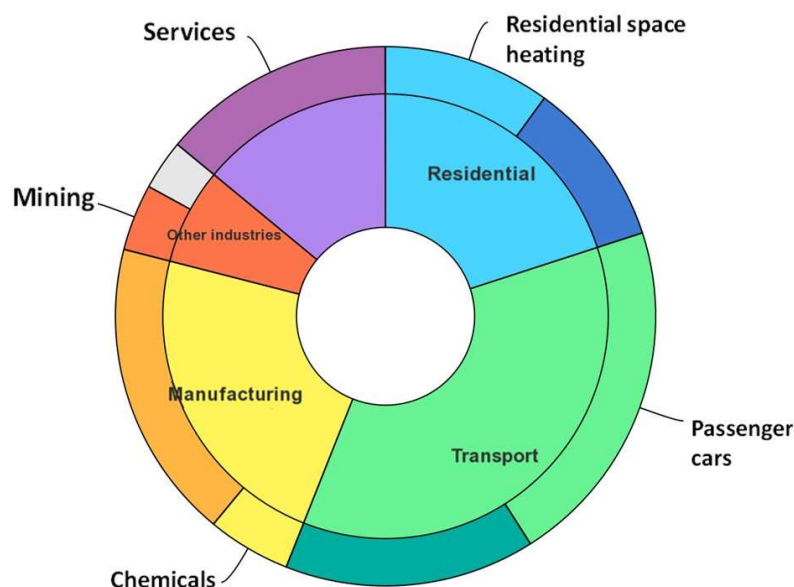


Figure 1. Largest end uses of energy by sector in selected IEA countries, 2018 [IEA (2021), Key World Energy Statistics 2021, IEA, Paris <https://www.iea.org/reports/key-world-energy-statistics-2021>], accessed on 15 September 2022.

Perovskites have gained much attention in various fields, such as solar cells [1], membrane reactors [2], fuel cells [3], H₂ production [4], water splitting [5], methane combustion and pollutant removal [6]. These are well-known for their outstanding opto-electronic properties. Perovskites are oxides with the general formula ABX₃, where A and B are cations of different atomic sizes. Precisely, A is a monovalent (I) or divalent (II) metal cation with a larger radius (e.g., Na, Sr, Ba, La etc.), while B represents the transition metal (e.g., Co, Ru, Au etc.) and X represents non-metallic elements (O, N, Cl, Br). The ideal perovskite has a cubic structure with A cations occupying the corners in a 12-fold coordination and B cations are in the center of the cube surrounded with oxygen anions. Because of their beneficial characteristics, such as high light absorption coefficients, the ability to tune band gaps and band edges by replacing the cations in the structure or creating oxygen vacancies, these are thermodynamically feasible to produce hydrogen in an environmental-friendly way. In contrast to the traditionally used semiconductors, such as titania and other TiO₂-based materials, strontium titanate (SrTiO₃) can offer a number of advantages in photocatalytic applications. The strontium ions in SrTiO₃ can promote the formation of superoxide radicals, thus inhibiting the recombination of photogenerated charge carriers, which can facilitate the initiation of photocatalytic oxidation. In order to overcome some disadvantages, several attempts have been made to increase the photocatalytic activity of SrTiO₃ photocatalysts, by doping or deposition of metal nanoparticles, or by morphological and crystal plane modifications [7]. Most importantly, the cost involved in using perovskite-based materials is much lower, compared to Si- or Cu-based materials, for instance in solar panels, which would be advantageous for large-scale production. The alkaline earth titanates are perovskite oxides popular with their photocatalytic activity due to their band gaps. These consist of strontium, barium and calcium titanate (Sr, Ba, Ca) and

this review will focus on the strontium titanates potential in hydrogen generation and the photodegradation of organic pollutants (see Figure 2).

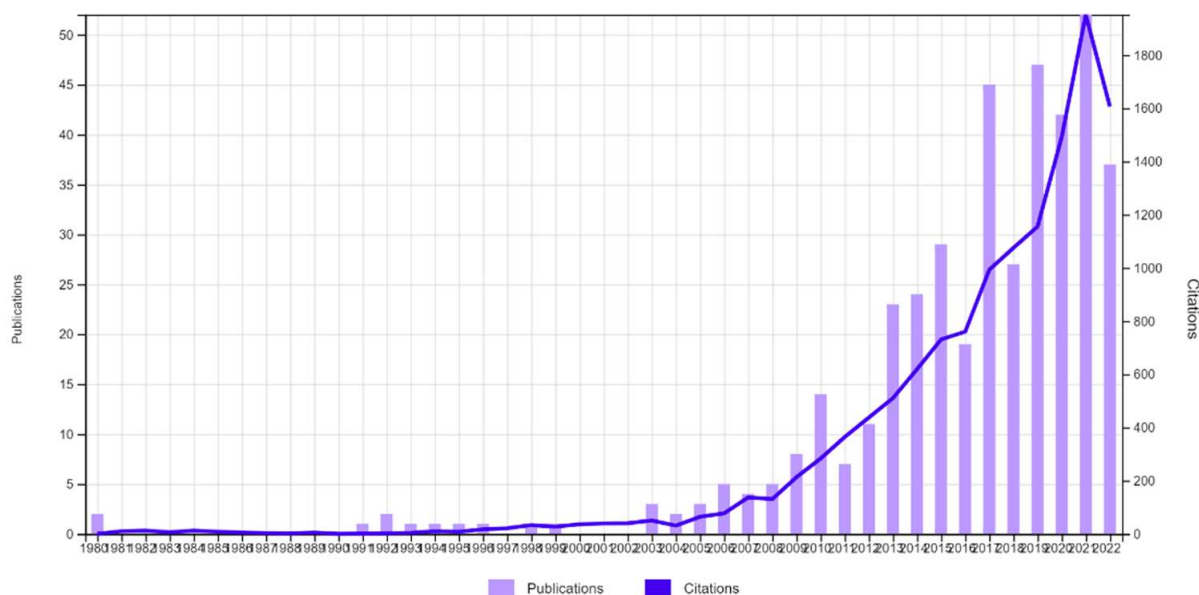


Figure 2. The number of relevant publications and citations [WoS Citation Report: photocat* (Topic) AND “strontium titanate” (All Fields)].

2. Properties of SrTiO₃

Strontium titanate (SrTiO₃) is a dielectric material that belongs to the class of “perovskites”. Structure-wise, SrTiO₃ is composed of TiO₆, octahedral at the corners with all 12 interstitial sites occupied by Sr, see Figure 3. It has a wide band gap (3.2 eV). It consists of valence orbitals Ti 3d and O 2p orbitals over to a Fermi surface. At room temperature, SrTiO₃ has a cubic structure (*Pm3m* space group) but it can undergo a phase transition into a tetragonal structure (*P4mm* space group) when it is cooled down to $-168\text{ }^{\circ}\text{C}$ [8]. It is an important material in the electronics industry because of its high dielectric constant. Studies have also reported its photocatalytic abilities in removing organic pollutants, and solar water splitting under UV irradiation. Due to its tunable band gap and good chemical and thermal stability, it has a greater capacity in hydrogen production. However, as mentioned, its wide band gap and fast recombination of electrons and holes restrict its use in photocatalysis under visible light, alone. Therefore, many modifications, such as doping with metals, non-metals or other semiconductors, have been adopted to solve these issues.

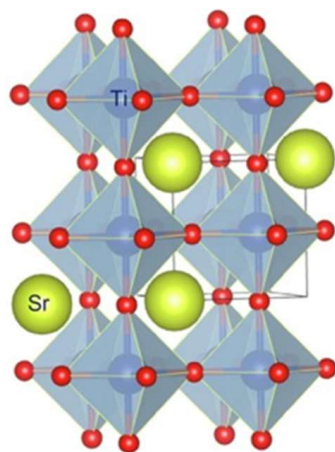


Figure 3. Structure of SrTiO₃ (cubic) [2]. Reprinted/adapted with permission from Elsevier, 2016.

With respect to the potential (photo)catalytic activity, the dominance of the individual crystal faces and the surface arrangement of the atoms forming the lattice are of great importance. Eglitis et al. reported a systematic study of the ab initio calculations for the series of ABO_3 perovskite (001) surfaces [9]. Based on the literature data, they also reviewed the experimental temperatures of the transition from the low-temperature phases to the high-temperature cubic structure, the corresponding experimental lattice parameters and the experimentally estimated band gap energies. (For $SrTiO_3$, the transition temperature into a cubic phase was 110 K, the band gap at RT was 3.25 eV (indirect) and the lattice constant was 3.9053 Å at 293 K.) Based on the B3LYP and B3PW calculations, another theoretical study has provided comparative data for the $YAlO_3$, $SrTiO_3$, $BaTiO_3$ and $BaZrO_3$ (001) and (111) surfaces [10]. The surface energies (in electron volts per surface cell) calculated for the $SrTiO_3$ (001) surfaces, were as follows: SrO-terminated—1.15, TiO_2 -terminated—1.23, and the variety of the optical band gaps for the different surfaces was also discussed. In a recent paper, Rusevich et al. highlighted the role of oxygen vacancies in perovskite crystals, on the structural, electronic and vibrational properties of $SrTiO_3$ [11]. Oxygen vacancies have been shown to have no noticeable effect on the macroscopic crystal structure, but alter its electronic and vibrational properties. It has been also observed that the reduction of oxygen gives rise to new local vibrational modes at frequencies that are absent in stoichiometric bulk crystals. The surface properties of $SrTiO_3$ are very important, from the catalysis perspective. There are many studies reported in the literature concerning the $SrTiO_3$ (100) surface properties. The (100) surface of $SrTiO_3$ is known to be more stable and much easier to prepare than (110) and (111) surfaces. For the photocatalytic degradation of the organic pollutants, the {100} surface works best while for the hydrogen evolution, the {110} surface facets is the most active phase. The optical and photocatalytic properties are facet-dependent. Hseih et al. recently studied the necessity of incorporating tunable degrees of the surface-dependent band bending [12]. The {110} facets are much more efficient for the hydrogen production reaction since it facilitates the migration of the photoexcited electrons to this surface which promotes the H^+ reduction to produce H_2 gas. The study by Qiang et al. showed that the TiO_2 -terminated surface behaves very differently from the SrO-terminated one and that the surface structure is a sensitive function of the oxygen partial pressure and temperature [13]. These studies show that the careful designing of the facets of the photocatalyst may lead to an efficient photocatalyst for photocatalytic applications.

3. Different Synthesis Methods for $SrTiO_3$

$SrTiO_3$ can be prepared using different methods, such as hydrothermal, sol gel, co-precipitation, solid-state reaction, ultrasound and microwave-assisted synthesis. All of the above-mentioned methods have advantages and serious drawbacks. For instance, although solid-state synthesis is suitable for a large scale production, it results in lower surface areas with larger particle sizes and high amounts of impurities. Moreover, the sol gel process requires a lower calcination temperature and the hydrothermal method results in highly crystalline structures and reduced amounts of impurities. Some of the examples of the $SrTiO_3$ synthesis with different methods are reported in Table 1.

Table 1. Different synthesis methods used for the preparation of the $SrTiO_3$ nanoparticles.

Synthesis Type	Precursors Used	Particle Size	Key Findings of the Work	Ref.
solid state	$SrCO_3$, TiO_2 , Bi_2O_3 , Na_2CO_3	not applicable	single crystals of mixed titanate oxides with Sr, were obtained	[14]
room temperature	$Sr(OH)_2 \cdot 8H_2O$, hydrous titania gel	80–100 nm	high crystallinity at a low temperature, in the absence of solvents/additional reagents	[15]

Table 1. Cont.

Synthesis Type	Precursors Used	Particle Size	Key Findings of the Work	Ref.
solvothermal	$\text{Sr}(\text{NO}_3)_2$, H_2TiO_3	20–30 nm	growth of the SrTiO_3 nanocrystallites was very sensitive to the EtOH:H ₂ O ratio; a 1:1 ratio resulted in the crystal formation of SrTiO_3	[16]
sol gel	$\text{Sr}(\text{NO}_3)_2$, titanium isopropoxide, citric acid	~39 nm	SrTiO_3 nanorods with an enhanced photocatalytic activity was obtained	[17]
hydrothermal	$\text{Sr}(\text{OH})_2 \cdot 8\text{H}_2\text{O}$, titanium(IV) bis(ammonium lactato)dihydroxide (TALH)	20–40 nm	SrTiO_3 nanoparticles prepared at low temperatures, compared to the conventional methods, exhibited a large surface area and the highest degradation rate for NO gas	[18]
microwave aided thermal	strontium titanyl oxalate hydrate $\text{SrTiO}(\text{C}_2\text{O}_4)_2 \cdot 4\text{H}_2\text{O}$ (STO)	28–68 nm	cubic SrTiO_3 nanopowders synthesized at a low temperature and in a shorter period of time resulted in a smaller particle size	[19]

The types and conditions of the synthesis has a huge impact on the morphology and surface properties of the final product. Interestingly, neither the particle size nor the band gap value was significantly affected by the synthesis method, as can be concluded from Table 1's data. Only one publication has reported a slightly higher particle size, around 100 nm, which was associated with a high degree of crystallinity. The production strategies listed in the table did not result in significant differences in the band gap values. In all cases, a value of around 3.2 eV was reported. Therefore, the precise control of the shape and size would help in fabricating high-performance material, such as those as photocatalysts [20]. Semiconductors with a highly crystallinity are more demanding in photocatalysis applications, since the increased crystallinity results in a decreased number of crystal defects, that act as the recombination center for the photogenerated electron and holes. Likewise, larger specific surface areas of the photocatalysts are beneficial as more active sites can be found, which further enhance the adsorption of the pollutant on the photocatalyst surface. This is why it is important to carefully choose the conditions for their synthesis [21]. In addition to the shape and size-dependent photoreactivity, it was seen that the band gap (E_g) of SrTiO_3 varied when different methods and processing details were used. For instance, the band gap for the SrTiO_3 nanoparticles prepared using the hydrothermal method, was around 3.10 eV, while the band gap was nearly 2.00 eV when the ball milling method was used [20,22]. It was suspected that this difference in the band gap values is due to the presence of certain impurities. Another study reported E_g as 3.35 eV of the SrTiO_3 nanoparticles, using a co-precipitation method [23]. Some of the commonly used methods are briefly discussed in this section.

The solid-state reaction method is basically a “solvent-less” reaction, where the precursors react chemically in the absence of solvents. This means an economically feasible way and no waste generation and therefore, it is environmentally-friendly in nature. In addition, the ball miller is used in this synthesis, to homogenize the samples and obtain particles in the nano-range. Another significance of an additional milling step is to prevent the formation of secondary phases during the calcination process. The most important factors to consider are the milling speed and time because these factors could easily modify the morphology of the samples. Hence, the careful tuning of these factors could result in the desired morphology. For the SrTiO_3 synthesis, the low cost of the precursors, together with the simplicity of this process, makes it ideal, from an industrial perspective. However,

the use of higher temperatures during the calcination step is a serious drawback as it not only leads to the particle agglomeration, but also to a lower surface area, and the high level of impurities are unavoidable. For the precursors, usually titanium dioxide is used as a titanium source, and salts of strontium as carbonates or nitrates, serve as the strontium source. Interestingly, the nature of the strontium salt used drastically affects the temperature conditions for the calcination. For instance, the study by Kumada et al. showed that the use of nitrate precursors drastically reduced the temperature requirements to 600–700 °C, in comparison to the carbonate salt where temperatures as high as 1300 °C were used [24].

The hydrothermal method is the most common and versatile method. In this method, the reaction is carried out in an enclosed stainless steel vessel at specific temperatures for a desired period. It offers a better control of the morphology, size and crystallinity, which has a direct impact on the catalytic performance of the product. The temperature conditions and the volume of solvent used, decides the shape and size of the material. Moreover, the step of calcination is eliminated in this method, which gives an additional superiority over the solid-state method. A variety of titanium compounds are used for the hydrothermal synthesis of SrTiO₃, such as rutile and/or anatase TiO₂ [25], tetrabutyl titanate, amorphous titanium hydroxide [26], titanium (IV) i-propoxide [27–29] and titanium (IV) n-propoxide [30]. For a hydrothermal synthesis of the alkaline earth metal titanates, the process starts with the hydrolysis of the titanium source (in alkaline media) in presence of an alkaline earth metal salt. The very popular theory for the SrTiO₃ synthesis via hydrothermal synthesis, is a “dissolution-precipitation” process. According to this, the process begins with the formation of the strontium ions from the hydrolysis of the strontium precursor, followed by the reaction with the Ti-precursor with hydroxide ions, to form soluble [Ti(OH)₆]²⁻ complexes. A new SrTiO₃ phase is produced as a result of the mutual integration and precipitation of the strontium ion and [Ti(OH)₆]²⁻ complexes. Many researchers have also reported doped-SrTiO₃ from the hydrothermal synthesis [21,31,32].

One of the critical point observed during the SrTiO₃ hydrothermal synthesis was the appearance of a secondary phase SrCO₃ (orthorhombic), along with SrTiO₃. It is predicted that the CO₂ in the air during the pre/post-treatment, would dissolve as CO₃²⁻ in the mixture and slowly reacts with the Sr²⁺ ions coming from the precursor. Even if the concentration of CO₂ is too low, the formation of this solid with a low solubility can occur. However, a study showed that by applying mechanical stirring, the appearance of SrCO₃ can be avoided [33]. Moreover, in certain cases, the presence of SrCO₃, together with SrTiO₃, has boosted the overall photocatalytic efficiency of the composites, as reported by Biborka et al. [34]. In a nutshell, it can be said that we can benefit from the presence of secondary phases, such as SrCO₃, under specific conditions.

The sol-gel method is one of the methods widely employed for producing different oxide compounds or for the synthesis of nanomaterials. The process involves the controlled hydrolysis of metal alkoxides, to form a solution and then a gel formation. This is further followed by a high temperature treatment, to induce polymerization and finally a metal-oxide network. However, the demerits of the process, such as the expensive metal alkoxide precursors and calcination at high temperatures, pose certain limitations on the applicability of the process, on a large scale.

In addition to the methods discussed previously, researchers have also reported the combination of processes, to overcome the limitations of one process with the advantageous parts of another process. For instance, the Rh doped SrTiO₃ with a high crystallinity, was prepared using the microwave-assisted hydrothermal method for the hydrogen evolution [35]. The SrTiO₃ nanocrystals, free from any by-products, were formed at a very low synthesis temperature by using the sonochemical method [36]. Similarly, in another study, the ultrasonic-assisted hydrothermal synthesis of the Ni-doped SrTiO₃, the ultrasonication played a significant role in homogenizing the dispersed nanoparticles. Another example where the combination of the hydrothermal synthesis with the calcination, was reported by Zhao et al. [37]. More studies can be found on the combination of different synthesis

methods, which has benefitted SrTiO₃ in enhancing the structural, morphological or optical properties, which indirectly affects their performance in different applications (hydrogen production, pollutant removal, NO reduction, etc.), such as those reported in [38–40].

Year after year, several advancements have been made, to drive the efficiency of the SrTiO₃-based photocatalysts into visible light. Due to the wide band gap of SrTiO₃, it is very difficult to obtain visible light catalytic activity and measures, such as doping, which are taken to modify its band gap. Its perovskite structure provides an advantage to accommodate the dopants and introduce some defects, which enhance the interaction with the adsorbed molecules. Doping with the metal cations into the bulk, facilitates the formation of new energy levels in the band gap. Not only does it modify the band structure, but it also suppresses the recombination of electrons and holes. For the hydrogen generation under visible light, the most common dopants reported include Mn [41], Fe [42], Cr [43,44], Rh [45,46], Pb, Ag and Au. Saadetnejad et al. doped SrTiO₃ with Au and Al for hydrogen production [47]. The study dealt with the effect of the doping amount of Au and Al and the concentration of the sacrificial agents on the overall yield of hydrogen. The highest hydrogen production rate was obtained by a sample of 0.25% Au-1.0% Al/SrTiO₃, at different concentrations of the sacrificial agents. Similarly, Eu-doped strontium zirconate titanate was prepared for H₂ production and the best performance was obtained under an alkaline condition with a higher concentration of sacrificial agents, such as EDTA [48]. Similarly, doping with rare earth elements, such as cerium (Ce), is becoming popular as the effective separation of the photogenerated charge carriers was observed, for instance, in the study of Xie et al., where doping with Ce resulted in capturing electrons by Ce⁴⁺, thus inhibiting the recombination of electrons and holes and enhancing the quantum efficiency of SrTiO₃ [49]. Numerous examples could be seen in the literature, on the successful doping of SrTiO₃, for improving its catalytic performance. Some of them are listed in the Table 2.

Table 2. Studies on the doping of strontium titanate with different metals and transition metals.

Designed Photocatalyst	Application	Determining Factors of the Study	Ref.
In-doped SrTiO ₃	water splitting	substitution of the Ti ⁴⁺ cations by In ³⁺ at the B site	[50]
Se and Te- doped SrTiO ₃	hydrogen production	band gap narrowing due to the decreased ionic strength of the Sr-O bonds and the increased covalency strength of the Ti-O bonds on the doping	[51]
N ₂ -doped TiO ₂ -SrTiO ₃	rhodamine B (Rh B) dye photodegradation	red-shift of the absorption edge upon the nitrogen doping leading to the band gap reduction	[52]
Cr-doped SrTiO ₃	hydrogen evolution	Cr dopants replaced the Ti sites, an excellent charge transfer and separation efficiency, owing to a single crystal	[53]
g-C ₃ N ₄ /SrTiO ₃	hydrogen production	interfacial coupling between g-C ₃ N ₄ and SrTiO ₃ by forming the type II heterojunction and the built-in electric field in the interface	[54]
Au and Rh-doped SrTiO ₃	syngas production	interband transmission of Au and the role of Rh as a photoelectron accumulator and CH ₄ reforming	[55]
Eu-doped SrTiO ₃	Rh B degradation	formation of smaller particles with a higher surface area	[56]

Table 2. Cont.

Designed Photocatalyst	Application	Determining Factors of the Study	Ref.
Cr-doped SrTiO ₃	Cr (VI) removal	substitution of Cr ³⁺ for Sr ²⁺ resulted in the red-shift of the absorption edge, visible to light, nanoplate morphology a with larger surface area obtained	[57]
Fe-doped SrTiO ₃	dibutyl phthalate	decreased average crystallite size with a narrow band gap	[58]
Cu-doped SrTiO ₃	selective alcohol oxidation of benzyl alcohol into benzyl aldehyde	Cu dopants induce abundant oxygen vacancies and introduce the inter-band springboard into SrTiO ₃ , imparting a response under visible light and near the infrared region	[59]
La/Cr co-doped SrTiO ₃	hydrogen production	light absorbance and catalytic performance are strongly governed by the Ti-O bond length and the Ti-O-Ti bond angle	[60]
N-doped SrTiO ₃	dye degradation (methylene blue, methyl orange and RhB)	use of glycine resulted in a mesoporous structure, besides a higher surface area, due to N-doping and oxygen vacancy	[61]
SrTiO ₃ doped with Na ions	water splitting	introduction of the NA ions induced a crystal deformation and oxygen vacancies	[62]

4. Applications

The perovskite structures are in demand, especially, in the solar panel fabrication, due to their low cost, high efficiency and lightweight, in comparison to the conventional photovoltaic materials, such as silicon [63]. SrTiO₃, as discussed before, comes under the category of perovskite structures and recently increased number of studies are reported on their modifications and further applications in energy storage and environmental remediation, such as solar cells, hydrogen production, selective oxidation of alcohols, pollutant removal by photodegradation, etc.

4.1. SrTiO₃ in Hydrogen Production

Hydrogen, as we know, is the most abundant element on the planet and its high energy content with carbon-free emissions makes it environmentally benign. This is the reason why most of the studies on environmental remediation and energy storage are concerned with hydrogen production, to find an alternative to our non-renewable sources, such as fuel. Its future applications are expected to be in the sector of heating sources for both commercial and residential areas and for power generation. However, its production process consumes a high amount of energy. Until now, as discussed before, the generation of hydrogen is mainly achieved by steam reforming fossil fuels, thereby releasing a mixture of carbon monoxide, H₂ and synthetic gas. This leads to an increase in the level of carbon emissions and thus, to global warming. This is why it is very important at this stage to look for new, feasible, and safe ways to produce hydrogen, to meet our growing energy requirements. Hydrogen generation from the splitting of water via solar energy is becoming a promising way for the replacement of fuel. For this, many semiconductor materials, including TiO₂ and other perovskite metal oxides, have shown potential. Among them, recently, strontium titanates and their modifications are some of the popular choices. This is due to its band edge positions that fulfil the prime requirement for hydrogen generation, i.e., the valence band maximum to be more positive than the water oxidation potential and the conduction band minimum to be more negative than the hydrogen reduction potential. However, its band gap is too wide that it only absorbs the UV light. Additionally, SrTiO₃ alone is not sufficient to split water to produce hydrogen. Back in 1979, a study by Yoneyama et al., about water splitting into hydrogen and oxygen, by reduced SrTiO₃ powders, but

the decomposition rate was reduced with the irradiation time [64]. Therefore, most of the studies that report a higher hydrogen efficiency include the modified SrTiO₃. For instance, the addition of a co-catalyst to SrTiO₃, has facilitated the hydrogen production, such as in a recent study by Liuyang et al. where ethylene glycol (EG) was used as a co-catalyst with SrTiO₃ [65]. The resulting photocatalyst not only resulted in a higher yield of hydrogen, but also maintained its stability of SrTiO₃ coated with EG, for over 32 h. The overall yield was found to be 19.5 times higher than SrTiO₃ alone. In another study by Xuan et al., SrTiO₃ loaded with CuO showed high rates for hydrogen evolution. CuO facilitates the separation of electrons and hole pairs [66]. Other studies concerning the modifications of SrTiO₃ for the photocatalytic hydrogen production are listed in Table 3.

Table 3. Doped SrTiO₃ for the photocatalytic generation of hydrogen.

Catalyst system	Amount of Hydrogen Evolution	Optimum Loading Amount	Medium	Influential Factor	Ref.
CuO-loaded SrTiO ₃	CuO/ SrTiO ₃ : 5811 μmol Pure SrTiO ₃ : 34 μmol	1.5 wt. % of CuO	Aqueous methanol solution	Decreased recombination rate of the electron/hole pairs, due to CuO loading	[66]
Reduced graphene oxide (RGO)_SrTiO ₃	334.68 $\mu\text{mol g}^{-1}$	6 wt. % of RGO	Formic acid/sodium formate	High surface area and more active sites	[67]
Au/Al-SrTiO ₃	347 $\mu\text{mol/h.g.cat}$	0.25% Au, 1% Al at different alcohol concentrations	Aqueous solution of methanol, ethanol and isopropyl alcohol	Al doping increased band energy of SrTiO ₃ , metallic Al showing plasmonic effects, similar to Au	[47]
Rh-doped SrTiO ₃	48.1 $\mu\text{mol h}^{-1}$	1 mol%	Aqueous methanol solution	Rh ⁴⁺ cations in the bulk and on the surface	[45]
Zn-doped SrTiO ₃	73.2 $\mu\text{mol h}^{-1}$	* NA	Aqueous methanol solution	Zn ions changed the crystal and band structures and significantly promoted the carrier mobility of the catalysts	[68]
Er ³⁺ doped SrTiO ₃	NA	5 mol%	Aqueous methanol solution	Er ³⁺ doping leads to the decrease of the band gap	[69]
Mn-doped SrTiO ₃ /Carbon Fiber	267.69 $\mu\text{mol/g h}$	5% Mn	Mixture of Na ₂ S and Na ₂ SO ₃	Mn doping and oxygen vacancies extended the light absorption boundary to the visible light direction	[41]
Ag/SrTiO ₃	400 $\mu\text{mol h}^{-1} \text{ g}^{-1}$	* NA	Aqueous ethanol solution	Silver nanoparticles (AgNPs) act as a sink for the photogenerated electrons, boosting up the separation of the charge carriers	[4]

* NA = Not applicable (not specified).

However, a recent study revealed that the shape-controlled synthesis of SrTiO₃ can also be a key for the highly efficient photocatalytic hydrogen production [70]. Using different ethylene glycol (EG) and water (H₂O) ratios, Zhou et al. successfully prepared porous 3D SrTiO₃ structures as follows. The applied hydrothermal synthesis selectively produced the following morphologies, as a function of the medium: (a) assembled nanoparticles (ANPs), (b) golf ball-like particles (GLPs), (c) star-like microspheres (SLMs), (d) sin-like microspheres (ULMs), (e) small flower-like microspheres (FLMs-S), and (f) large flower-like microspheres (FLMs-L). By analyzing the X-ray photoelectron and diffuse reflectance spectroscopy results, it has been demonstrated that the crystal defects formed, not only result in a reduction of the valence band, but also shift the conduction band to a negative

value. The assumed band structures of the three selected samples are presented in Figure 4a. Comparing the activity of the Pt-loaded SrTiO₃ photocatalysts in hydrogen production, it was concluded that the stability of the micro-nano hierarchical structure plays an important role, and the oxygen vacancies in the crystal hinder the charge-hole recombination, thus enhance the photocatalytic activity; the proposed mechanism can be seen in Figure 4b.

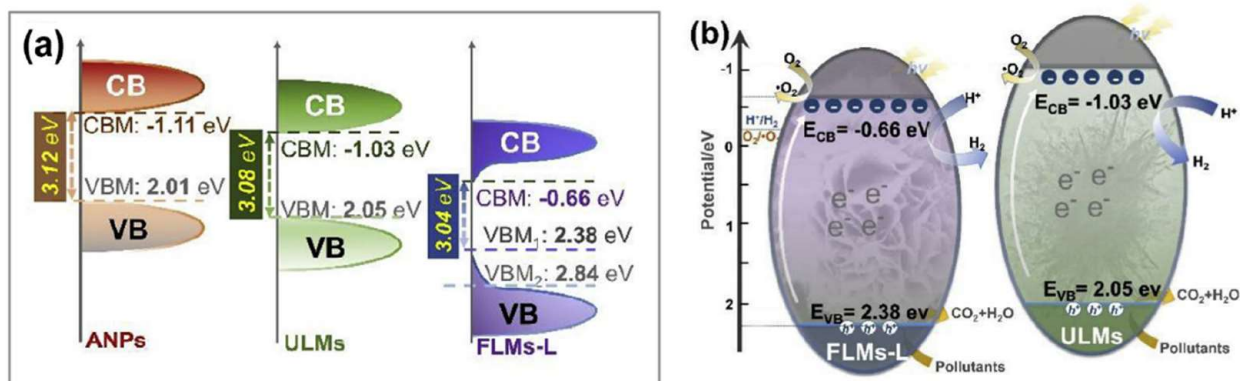


Figure 4. (a) Assumed band structures of the shape-controlled SrTiO₃ photocatalysts. (b) Proposed mechanism for the photocatalytic hydrogen evolution over the shape-controlled SrTiO₃ [70]. Reprinted/adapted with permission from Elsevier, 2019.

The other important point to consider is the different factors that can affect the hydrogen production efficiency of the strontium titanates.

4.2. Effect of the Calcination Time and Temperature

Calcination temperature is a very important factor that can remarkably affect the photocatalytic performance of SrTiO₃. This is because a number of properties, such as the surface area, porosity, adsorption rate or crystallization, can be affected by changes in the temperature conditions. Aizhong et al. studied the removal of malachite green dye by Ni,La-SrTiO₃ and reported the effect of the calcination temperature on the performance of SrTiO₃ [71]. The low calcination temperature resulted in a higher photocatalytic degradation due to the combination of the properties obtained, such as the large surface area and pore volume, a high visible light absorbing ability and high adsorption rates. The study of Hong et al. discloses their effect in the addition to the sulphur content, on the decomposition of methylene blue by SrTiO₃. Other than this, the heating rate during the crystallization process is also known to affect the overall efficiency of SrTiO₃. For instance, in the study of Luis et al. the lowest heating rate was found to result in the best photocatalytic activity of the SrTiO₃ nanoparticles for the methylene blue removal [72].

4.3. Effect of the Metal Type and Loading Concentration of the Metal

The effect of metal loading was seen on the light harvesting ability of SrTiO₃, however, no effects were seen on the physical properties of the material. The electrochemical properties of the doped-metal was the deciding factor. The thorough study of Tarawipa et al. summarizes the effect of using different metals (Au, Ni, Pt, Ag, Ce and Fe) [73]. The highest hydrogen efficiency was obtained by using Au at a loading of 1 wt.% while Ce and Fe had a negative effect on the hydrogen generation. Similarly, the addition of Na⁺ ion to SrTiO₃ using the impregnation method, led to the high photocatalytic activity of SrTiO₃ [74]. This effect can be presumed to be coming out from the effect of adding the Na⁺ ion which may be due to the substitution of the Sr⁺ ions and therefore, inducing similar effects, as in the case of the Na⁺ ion doping at the preparation step.

In some cases, the purity of the raw materials played an important role, for example, in the study by Junzhe et al. [62]. The enhanced photocatalytic activity for water splitting and the extended lifetime of the photogenerated charge carriers was attributed to the doping

by the Na^+ ions. The performance of the photocatalyst was dependent on the purity of the raw material rather than the ionic state obtained during the preparation method. Further, the preferable state for Na-SrTiO_3 was the doping of Na^+ , to the perovskite structure of SrTiO_3 . This is because Na^+ doping results in the oxygen vacancy, which may inhibit the formation of the entities that can act as the recombination center, such as Ti^{3+} , also reported by Takata et al. [75]

The advantage and drawback of SrTiO_3 in H_2 -production: strontium titanates are considered to be catalytically active when it comes to the application of water splitting. Although the band gap of SrTiO_3 is similar to TiO_2 (3.2 eV), the conduction band is more negative than TiO_2 , which makes it a good candidate for the hydrogen production application. However, the efficiency of pure SrTiO_3 is still too low for the hydrogen generation because of the fast recombination rate of the photogenerated electron/hole pairs. Hence, there is a need to modify SrTiO_3 , to obtain a high efficiency.

4.4. Photocatalytic Degradation of the Organic Pollutants

The application of the doped and undoped-strontium titanates has been largely examined for the degradation of the recalcitrant pollutants, such as dyes and pharmaceutical compounds, and the photoreduction of the Cr heavy metal. Gao et al. studied the photodegradation of the cationic and anionic dyes by the cubic SrTiO_3 [76]. The study revealed a significant finding about the influence of the synthesis conditions (time and temperature) and pH on the removal efficiency of the catalyst for the dyes. The prolonged hydrothermal time greatly influenced the morphology and the structural properties favoring the higher photocatalytic efficiency of SrTiO_3 . Interestingly, the cationic dye degradation is favored over the anionic dyes at a high pH. Another extensive study by Jakub et al. provided a holistic approach on the evaluation of the photocatalytic performance of different oxides, based on an organic matrix, rather than on one model contaminant [77]. The study was conducted on a mixture of contaminants containing 26 pharmaceutical compounds, classified as a model group of contaminants for the study and reported SrTiO_3 as one of the novel oxide compounds, besides TiO_2 , WO_3 and Bi_2O_3 , that enhanced the overall photodegradation process. Galloni et al. investigated the commercial powder of SrTiO_3 in nano- and micro-sizes, to determine the size effect on their photocatalytic efficiency [78]. The promising results were obtained for the diclofenac photodegradation with more than a 90% efficiency, within one hour under solar light. The composite of SrTiO_3 with $\text{Bi}_5\text{O}_7\text{I}$, reported a 12.5 and 3.97 times higher photocatalytic efficiency than their pristine form, for the degradation of the RhB dye under simulated solar light irradiation [79]. The nanocubes of SrTiO_3 decorated with CdS microspheres was studied by Guoling et al. for five different antibiotic degradations, under visible light [80]. Due to the formation of the heterojunctions, there exists an interfacial interaction between CdS and SrTiO_3 that was responsible for the enhanced separation of the electrons and hole pairs. The presence of CdS extended the absorption edge of SrTiO_3 from 380 nm to 580 nm, indicating the absorption under visible light. The highest degradation efficiency was obtained for ciprofloxacin. In a recent study, Bi-doped SrTiO_3 was synthesized using a solid-state method for the removal of acid orange 7 dye under visible light [81]. The doped samples showed a higher performance for the degradation of the dye than the undoped with the optimal amount of doping, in the case of sample $\text{Sr}_{0.95}\text{Bi}_{0.05}\text{TiO}_3$. It was presumed that the appearance of the secondary phase ($\text{Bi}_4\text{Ti}_3\text{O}_{12}$) might also play an important role in enhancing the degradation efficiency of the composite. In another study, da Silva et al. investigated the influence of the heating rate on the SrTiO_3 nanoparticles during calcination and how this affects the photocatalytic decomposition of methylene blue, rhodamine B and methyl orange dyes, in the presence of different scavengers, and they also proposed a degradation mechanism [72]. The direct photodegradation mechanism was assumed as the main pathway in the decomposition of the model organic pollutants catalyzed by the SrTiO_3 nanoparticles, see schematic diagram (Figure 5). Since the oxidative radicals are not generated under these circumstances, the holes forming in the valence band directly attack the MB dye. It has also been shown that

an electron acceptor (e.g., Ag^+) present in the conduction band is able to trap electrons, thereby improving the photoactivity of the SrTiO_3 sample and inhibiting the undesirable charge carrier recombination. Since the photocatalytic degradation processes are generally non-selective, it is likely that the suggested mechanism is valid for other organic pollutants as well.

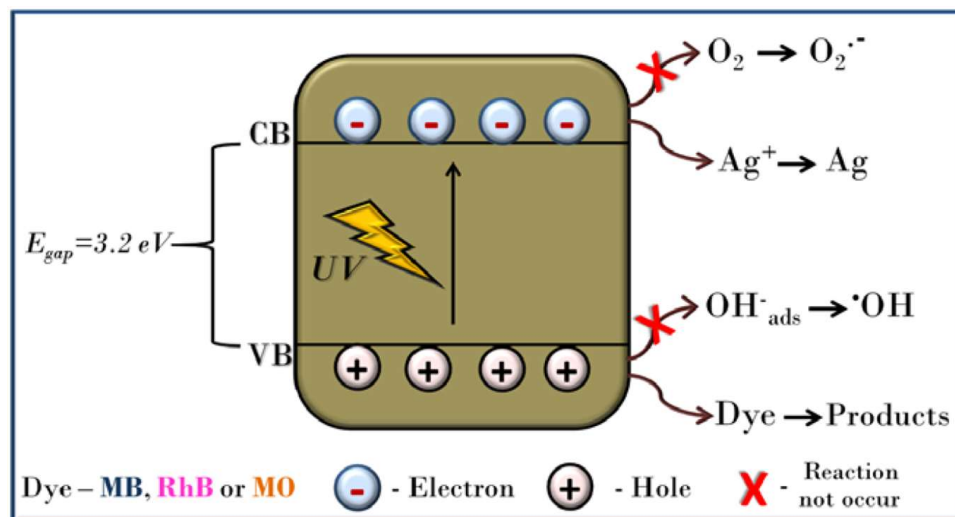


Figure 5. Plausible mechanism for the photocatalytic reaction catalyzed by the SrTiO_3 photocatalysts [72]. Reprinted/adapted with permission from John Wiley and Sons, 2009.

5. Conclusions

The perovskite-based materials are promising candidates for current science and technology, as their multifarious structures make them suitable for a wide range of applications. In summary, SrTiO_3 has also shown the significant potential in the areas of environmental protection and energy storage. Several promising results indicate that SrTiO_3 has the ability to split water and remove the toxic pollutants from wastewater. This review briefly summarizes the structural aspects of strontium titanates and various synthesis methods used for their preparation.

Among the key findings, it is important to mention that there can be significant differences between the “theoretical” perovskite structure and the structure of the experimentally produced efficient photocatalysts. The surface of the (photo)catalytically active semiconductors often contains defect sites, which may be beneficial for the adsorption of the model compound, to prolong the lifetime of the formed charge pair or to facilitate the activation step. The theoretical calculations that model the SrTiO_3 crystal plane provide much information for understanding these processes [9]. In the last decade, innovative synthesis methods (e.g., solid state, room temperature, solvothermal, sol gel, hydrothermal, microwave assisted) have undergone a great development, which has allowed the fine tuning of the properties of the synthesized semiconductor particles, thus allowing the design of their photocatalytic properties [6]. At the same time, the rapid improvement of analytical techniques provides increasingly precise feedback on the properties of the samples (such as morphology, specific surface area, purity impurities, surface structure, etc.), thus helping to reveal the key parameters in photocatalysis. Recent years have also brought major advances in the development of doped and (nano)composite strontium titanates. These new structures are capable of a more efficient light absorbance, alteration of the semiconductor band structure, interfacial coupling between components, increase in the average grain size and/or specific surface area, stabilization of the structure, increase in the number of photocatalytically active defect sites, etc. [47].

Further, the two most important applications, i.e., hydrogen production and the photocatalytic degradation of the organic pollutants were discussed. Unfortunately, a real quantitative comparison of both the photocatalytic degradation of the organic pollutants

and the hydrogen production processes is difficult to make in the absence of appropriate standards (including photocatalytic test conditions, the nature of model pollutants and many others). The majority of the works could report the high efficiency of SrTiO₃ only under the UV light region. However, the modified SrTiO₃ via doping are one of the popular choices adopted to extend their light absorption ability under the visible region. Many authors attribute the enhanced photocatalytic efficiency of strontium titanates to the amount of the aggregation-free dopant metal [42], the role of oxygen vacancies [51] the morphology [70], or even the stable structure with a high specific surface area [46], but unfortunately no general conclusion can be drawn from this at present. The obtained efficiencies, even after doping, are still too low from the industrial point of view.

Regarding future tendencies, it is very likely that strontium titanate is a worthy candidate for further similar research, sooner or later, even for industrial applications. The dynamically evolving studies so far have made it clear (see Figure 2) that both the doping/composite formation and modification of the morphology/specific surface area/stability or a combination of these parameters could provide a number of breakthrough results in the near future.

Author Contributions: Conceptualization, N.S.; writing—original draft preparation, N.S.; writing—review and editing, K.H.; supervision, K.H. All authors have read and agreed to the published version of the manuscript.

Funding: This research received no external funding.

Data Availability Statement: Not applicable.

Conflicts of Interest: The authors declare no conflict of interest.

References

1. Neophytou, M.; De Bastiani, M.; Gasparini, N.; Aydin, E.; Ugur, E.; Seitkhan, A.; Moruzzi, F.; Choai, Y.; Ramadan, A.J.; Troughton, J.R.; et al. Enhancing the Charge Extraction and Stability of Perovskite Solar Cells Using Strontium Titanate (SrTiO₃) Electron Transport Layer. *ACS Appl. Energy Mater.* **2019**, *2*, 8090–8097. [CrossRef]
2. Olivier, L.; Haag, S.; Mirodatos, C.; Van Veen, A.C. Oxidative coupling of methane using catalyst modified dense perovskite membrane reactors. *Catal. Today* **2009**, *142*, 34–41. [CrossRef]
3. Burnat, D.; Heel, A.; Holzer, L.; Kata, D.; Lis, J.; Graule, T. Synthesis and performance of A-site deficient lanthanum-doped strontium titanate by nanoparticle based spray pyrolysis. *J. Power Sources* **2012**, *201*, 26–36. [CrossRef]
4. Ramos-Sanchez, J.E.; Camposeco, R.; Lee, S.-W.; Rodríguez-González, V. Sustainable synthesis of AgNPs/strontium-titanate-perovskite-like catalysts for the photocatalytic production of hydrogen. *Catal. Today* **2020**, *341*, 112–119. [CrossRef]
5. Phoon, B.L.; Lai, C.W.; Pan, G.-T.; Yang, T.C.-K.; Juan, J.C. One-pot hydrothermal synthesis of strontium titanate nanoparticles photoelectrode using electrophoretic deposition for enhancing photoelectrochemical water splitting. *Ceram. Int.* **2018**, *44*, 9923–9933. [CrossRef]
6. Gurav, H.R.; Bobade, R.; Das, V.L.; Chilukuri, S. Carbon dioxide reforming of methane over ruthenium substituted strontium titanate perovskite catalysts. *Indian J. Chem. Sect. A Inorg. Phys. Theor. Anal. Chem.* **2012**, *51*, 1339–1347.
7. Gyulavári, T.; Dusnoki, D.; Márta, V.; Yadav, M.; Abedi, M.; Sági, A.; Kukovecz, Á.; Kónya, Z.; Pap, Z. Dependence of Photocatalytic Activity on the Morphology of Strontium Titanates. *Catalysts* **2022**, *12*, 523. [CrossRef]
8. Ekuma, C.E.; Jarrell, M.; Moreno, J.; Bagayoko, D. First principle electronic, structural, elastic, and optical properties of strontium titanate. *AIP Adv.* **2012**, *2*, 012189. [CrossRef]
9. Eglitis, R.; Popov, A. Systematic trends in (0 0 1) surface ab initio calculations of ABO₃ perovskites. *J. Saudi Chem. Soc.* **2018**, *22*, 459–468. [CrossRef]
10. Eglitis, R.; Purans, J.; Popov, A.I.; Jia, R. Systematic trends in YAlO₃, SrTiO₃, BaTiO₃, BaZrO₃ (001) and (111) surface ab initio calculations. *Int. J. Mod. Phys. B* **2019**, *33*, 1950390. [CrossRef]
11. Rusevich, L.L.; Kotomin, E.A.; Zvejniaks, G.; Popov, A.I. Ab initio calculations of structural, electronic and vibrational properties of BaTiO₃ and SrTiO₃ perovskite crystals with oxygen vacancies. *Low Temp. Phys.* **2020**, *46*, 1185–1195. [CrossRef]
12. Hsieh, P.-L.; Naresh, G.; Huang, Y.-S.; Tsao, C.-W.; Hsu, Y.-J.; Chen, L.-J.; Huang, M.H. Shape-Tunable SrTiO₃ Crystals Revealing Facet-Dependent Optical and Photocatalytic Properties. *J. Phys. Chem. C* **2019**, *123*, 13664–13671. [CrossRef]
13. Li, Z.-Q.; Zhu, J.-L.; Wu, C.Q.; Tang, Z.; Kawazoe, Y. Relaxations of TiO₂- and SrO-terminated SrTiO₃(001) surfaces. *Phys. Rev. B* **1998**, *58*, 8075–8078. [CrossRef]
14. Lee, D.; Vu, H.; Sun, H.; Pham, T.L.; Nguyen, D.T.; Lee, J.-S.; Fisher, J.G. Growth of (Na_{0.5}Bi_{0.5})TiO₃-SrTiO₃ single crystals by solid state crystal growth. *Ceram. Int.* **2016**, *42*, 18894–18901. [CrossRef]

15. Yamaguchi, Y.; Kanamaru, Y.; Fukushima, M.; Fujimoto, K.; Ito, S. Preparation of Highly Crystallized Strontium Titanate Powders at Room Temperature. *J. Am. Ceram. Soc.* **2015**, *98*, 3054–3061. [[CrossRef](#)]
16. Wang, N.; Kong, D.; He, H. Solvothermal synthesis of strontium titanate nanocrystallines from metatitanic acid and photocatalytic activities. *Powder Technol.* **2010**, *207*, 470–473. [[CrossRef](#)]
17. Kiran, K.S.; Ashwath Narayana, B.S.; Lokesh, S.V. Enhanced Photocatalytic Activity of Perovskite SrTiO₃ Nanorods. *Solid State Technol.* **2020**, *63*, 1913–1920. Available online: <http://solidstatetechnology.us/index.php/JSST/article/view/2287> (accessed on 29 September 2022).
18. Kobayashi, M.; Suzuki, Y.; Goto, T.; Cho, S.H.; Sekino, T.; Asakura, Y.; Yin, S. Low-temperature hydrothermal synthesis and characterization of SrTiO₃ photocatalysts for NO_x degradation. *J. Ceram. Soc. Jpn.* **2018**, *126*, 135–138. [[CrossRef](#)]
19. Malghe, Y.S. Nanosized SrTiO₃ powder from oxalate precursor microwave aided synthesis and thermal characterization. *J. Therm. Anal.* **2010**, *102*, 831–836. [[CrossRef](#)]
20. Huang, S.-T.; Lee, W.W.; Chang, J.-L.; Huang, W.-S.; Chou, S.-Y.; Chen, C.-C. Hydrothermal synthesis of SrTiO₃ nanocubes: Characterization, photocatalytic activities, and degradation pathway. *J. Taiwan Inst. Chem. Eng.* **2014**, *45*, 1927–1936. [[CrossRef](#)]
21. Xu, J.; Wei, Y.; Huang, Y.; Wang, J.; Zheng, X.; Sun, Z.; Fan, L.; Wu, J. Solvothermal synthesis nitrogen doped SrTiO₃ with high visible light photocatalytic activity. *Ceram. Int.* **2014**, *40*, 10583–10591. [[CrossRef](#)]
22. Liu, Y.; Xie, L.; Li, Y.; Yang, R.; Qu, J.; Li, Y.; Li, X. Synthesis and high photocatalytic hydrogen production of SrTiO₃ nanoparticles from water splitting under UV irradiation. *J. Power Sources* **2008**, *183*, 701–707. [[CrossRef](#)]
23. Chen, Y.-H.; Chen, Y.-D. Kinetic study of Cu(II) adsorption on nanosized BaTiO₃ and SrTiO₃ photocatalysts. *J. Hazard. Mater.* **2011**, *185*, 168–173. [[CrossRef](#)] [[PubMed](#)]
24. Kumada, N.; Miura, A.; Takei, T.; Adilina, I.B.; Shimazu, S. Low temperature synthesis of ATiO₃ (A: Mg, Ca, Sr, Ba) by using molten salt. *J. Ceram. Soc. Jpn.* **2013**, *121*, 74–79. [[CrossRef](#)]
25. Zhang, Y.; Zhong, L.; Duan, D. Single-step hydrothermal synthesis of strontium titanate nanoparticles from crystalline anatase titanium dioxide. *Ceram. Int.* **2015**, *41*, 13516–13524. [[CrossRef](#)]
26. Boston, R.; Guo, J.; Funahashi, S.; Baker, A.L.; Reaney, I.M.; Randall, C.A. Reactive intermediate phase cold sintering in strontium titanate. *RSC Adv.* **2018**, *8*, 20372–20378. [[CrossRef](#)]
27. Nakashima, K.; Kera, M.; Fujii, I.; Wada, S. A new approach for the preparation of SrTiO₃ nanocubes. *Ceram. Int.* **2012**, *39*, 3231–3234. [[CrossRef](#)]
28. SLee, J.; Thiyagarajan, P.; Lee, M.J. Synthesis and characterization of strontium titanate powder via a simple polymer solution route. *J. Ceram. Process. Res.* **2008**, *9*, 385–388.
29. Jayabal, P.; Sasirekha, V.; Mayandi, J.; Jeganathan, K.; Ramakrishnan, V. A facile hydrothermal synthesis of SrTiO₃ for dye sensitized solar cell application. *J. Alloy. Compd.* **2014**, *586*, 456–461. [[CrossRef](#)]
30. Roque-Ruiz, J.-A.J. Sol-Gel Synthesis of Strontium Titanate Nanofibers by Electrospinning. *J. Ceram. Sci. Technol.* **2019**, *10*, 29–38. [[CrossRef](#)]
31. Wu, G.; Li, P.; Xu, D.; Luo, B.; Hong, Y.; Shi, W.; Liu, C. Hydrothermal synthesis and visible-light-driven photocatalytic degradation for tetracycline of Mn-doped SrTiO₃ nanocubes. *Appl. Surf. Sci.* **2015**, *333*, 39–47. [[CrossRef](#)]
32. Zhu, J.; Zhang, Y.; Shen, L.; Li, J.; Li, L.; Zhang, F.; Zhang, Y. Hydrothermal synthesis of Nb⁵⁺-doped SrTiO₃ mesoporous nanospheres with greater photocatalytic efficiency for Cr(VI) reduction. *Powder Technol.* **2022**, *410*, 117886. [[CrossRef](#)]
33. Mourão, H.A.; Lopes, O.F.; Ribeiro, C.; Mastelaro, V.R. Rapid hydrothermal synthesis and pH-dependent photocatalysis of strontium titanate microspheres. *Mater. Sci. Semicond. Process.* **2015**, *30*, 651–657. [[CrossRef](#)]
34. Boga, B.; Steinfeldt, N.; Moustakas, N.G.; Peppel, T.; Lund, H.; Rabeah, J.; Pap, Z.; Cristea, V. Strunk, Role of SrCO₃ on photocatalytic performance of SrTiO₃-SrCO₃ Composites. *Catalysts* **2022**, *12*, 978. [[CrossRef](#)]
35. Lin, H.-Y.; Cian, L.-T. Microwave-Assisted Hydrothermal Synthesis of SrTiO₃:Rh for Photocatalytic Z-scheme Overall Water Splitting. *Appl. Sci.* **2018**, *9*, 55. [[CrossRef](#)]
36. Ashiri, R.; Ajami, R.; Moghtada, A. Sonochemical Synthesis of SrTiO₃ Nanocrystals at Low Temperature. *Int. J. Appl. Ceram. Technol.* **2014**, *12*, E202–E206. [[CrossRef](#)]
37. Zhao, W.; Liu, N.; Wang, H.; Mao, L. Sacrificial template synthesis of core-shell SrTiO₃/TiO₂ heterostructured microspheres photocatalyst. *Ceram. Int.* **2017**, *43*, 4807–4813. [[CrossRef](#)]
38. Šetinc, T.; Spreitzer, M.; Vengust, D.; Jerman, I.; Suvorov, D. Inherent defects in sol-precipitation/hydrothermally derived SrTiO₃ nanopowders. *Ceram. Int.* **2013**, *39*, 6727–6734. [[CrossRef](#)]
39. da Silva, L.F.; Avansi, W.; Andrés, J.; Ribeiro, C.; Moreira, M.L.; Longo, E.; Mastelaro, V.R. Long-range and short-range structures of cube-like shape SrTiO₃ powders: Microwave-assisted hydrothermal synthesis and photocatalytic activity. *Phys. Chem. Chem. Phys.* **2013**, *15*, 12386–12393. [[CrossRef](#)]
40. da Silva, L.F.; Avansi, W.; Moreira, M.L.; Andrés, J.; Longo, E.; Mastelaro, V.R. Novel SrTi_{1-x}Fe_xO₃ nanocubes synthesized by microwave-assisted hydrothermal method. *CrystEngComm* **2012**, *14*, 4068–4073. [[CrossRef](#)]
41. Hu, Q.; Niu, J.; Zhang, K.-Q.; Yao, M. Fabrication of Mn-Doped SrTiO₃/Carbon Fiber with Oxygen Vacancy for Enhanced Photocatalytic Hydrogen Evolution. *Materials* **2022**, *15*, 4723. [[CrossRef](#)] [[PubMed](#)]
42. Ying, Z.; Chen, S.; Peng, T.; Li, R.; Zhang, J. Fabrication of an Fe-Doped SrTiO₃ Photocatalyst with Enhanced Dinitrogen Photofixation Performance. *Eur. J. Inorg. Chem.* **2019**, *2019*, 2182–2192. [[CrossRef](#)]

43. Rechberger, F.; Ilari, G.; Willa, C.; Tervoort, E.; Niederberger, M. Processing of Cr doped SrTiO₃ nanoparticles into high surface area aerogels and thin films. *Mater. Chem. Front.* **2017**, *1*, 1662–1667. [[CrossRef](#)]
44. Łącz, A.; Drożdż, E. Porous Y and Cr-doped SrTiO₃ materials—electrical and redox properties. *J. Solid State Electrochem.* **2019**, *23*, 2989–2997. [[CrossRef](#)]
45. Shen, P.; Lofaro, J.C.; Woerner, W.R.; White, M.G.; Su, D.; Orlov, A. Photocatalytic activity of hydrogen evolution over Rh doped SrTiO₃ prepared by polymerizable complex method. *Chem. Eng. J.* **2013**, *223*, 200–208. [[CrossRef](#)]
46. Murthy, D.H.K.; Matsuzaki, H.; Wang, Q.; Suzuki, Y.; Seki, K.; Hisatomi, T.; Yamada, T.; Kudo, A.; Domen, K.; Furube, A. Revealing the role of the Rh valence state, La doping level and Ru cocatalyst in determining the H₂ evolution efficiency in doped SrTiO₃ photocatalysts. *Sustain. Energy Fuels* **2018**, *3*, 208–218. [[CrossRef](#)]
47. Saadetnejad, D.; Yıldırım, R. Photocatalytic hydrogen production by water splitting over Au/Al-SrTiO₃. *Int. J. Hydrogen Energy* **2017**, *43*, 1116–1122. [[CrossRef](#)]
48. López-Vásquez, A.; Delgado-Niño, P.; Salas-Siada, D. Photocatalytic hydrogen production by strontium titanate-based perovskite doped europium (Sr_{0.97}Eu_{0.02}Zr_{0.1}Ti_{0.9}O₃). *Environ. Sci. Pollut. Res.* **2018**, *26*, 4202–4214. [[CrossRef](#)]
49. Xie, T.; Wang, Y.; Liu, C.; Xu, L. New Insights into Sensitization Mechanism of the Doped Ce (IV) into Strontium Titanate. *Materials* **2018**, *11*, 646. [[CrossRef](#)]
50. Sudrajat, H.; Fadlallah, M.M.; Tao, S.; Kitta, M.; Ichikuni, N.; Onishi, H. Dopant site in indium-doped SrTiO₃ photocatalysts. *Phys. Chem. Chem. Phys.* **2020**, *22*, 19178–19187. [[CrossRef](#)]
51. Bentour, H.; Boujnah, M.; Houmad, M.; El Yadari, M.; Benyoussef, A.; El Kenz, A. DFT study of Se and Te doped SrTiO₃ for enhanced visible-light driven photocatalytic hydrogen production. *Opt. Quantum Electron.* **2021**, *53*, 1–13. [[CrossRef](#)]
52. Ruzimuradov, O.; Sharipov, K.; Yarbekov, A.; Saidov, K.; Hojamberdiev, M.; Prasad, R.M.; Cherkashinin, G.; Riedel, R. A facile preparation of dual-phase nitrogen-doped TiO₂-SrTiO₃ macroporous monolithic photocatalyst for organic dye photodegradation under visible light. *J. Eur. Ceram. Soc.* **2015**, *35*, 1815–1821. [[CrossRef](#)]
53. Jiang, D.; Sun, X.; Wu, X.; Shi, L.; Du, F. Hydrothermal synthesis of single-crystal Cr-doped SrTiO₃ for efficient visible-light responsive photocatalytic hydrogen evolution. *Mater. Res. Express* **2019**, *7*, 015047. [[CrossRef](#)]
54. Luo, Y.; Deng, B.; Pu, Y.; Liu, A.; Wang, J.; Ma, K.; Gao, F.; Gao, B.; Zou, W.; Dong, L. Interfacial coupling effects in g-C₃N₄/SrTiO₃ nanocomposites with enhanced H₂ evolution under visible light irradiation. *Appl. Catal. B Environ.* **2019**, *247*, 1–9. [[CrossRef](#)]
55. Li, D.; Ouyang, S.; Xu, H.; Lu, D.; Zhao, M.; Zhang, X.; Ye, J. Synergistic effect of Au and Rh on SrTiO₃ in significantly promoting visible-light-driven syngas production from CO₂ and H₂O. *Chem. Commun.* **2016**, *52*, 5989–5992. [[CrossRef](#)]
56. Wang, Y.; Ma, W.; Song, Y.; Chen, J.; Xu, J.; Wang, D.; Mao, Z. Enhanced photocatalytic performance of SrTiO₃ powder induced by europium dopants. *J. Rare Earths* **2020**, *39*, 541–547. [[CrossRef](#)]
57. Yang, D.; Zhao, X.; Zou, X.; Zhou, Z.; Jiang, Z. Removing Cr (VI) in water via visible-light photocatalytic reduction over Cr-doped SrTiO₃ nanoplates. *Chemosphere* **2018**, *215*, 586–595. [[CrossRef](#)]
58. Abbas, H.A.; Jamil, T.S. Nano Sized Fe Doped Strontium Titanate for Photocatalytic Degradation of Dibutyl Phthalate under Visible Light. *Adv. Mater. Lett.* **2016**, *7*, 467–471. [[CrossRef](#)]
59. Li, B.; Hong, J.; Ai, Y.; Hu, Y.; Shen, Z.; Li, S.; Zou, Y.; Zhang, S.; Wang, X.; Zhao, G.; et al. Visible-near-infrared-light-driven selective oxidation of alcohols over nanostructured Cu doped SrTiO₃ in water under mild condition. *J. Catal.* **2021**, *399*, 142–149. [[CrossRef](#)]
60. Lu, L.; Ni, S.; Liu, G.; Xu, X. Structural dependence of photocatalytic hydrogen production over La/Cr co-doped perovskite compound ATiO₃ (A = Ca, Sr and Ba). *Int. J. Hydrogen Energy* **2017**, *42*, 23539–23547. [[CrossRef](#)]
61. Zou, F.; Jiang, Z.; Qin, X.; Zhao, Y.; Jiang, L.; Zhi, J.; Xiao, T.; Edwards, P.P. Template-free synthesis of mesoporous N-doped SrTiO₃ perovskite with high visible-light-driven photocatalytic activity. *Chem. Commun.* **2012**, *48*, 8514–8516. [[CrossRef](#)] [[PubMed](#)]
62. Jiang, J.; Kato, K.; Fujimori, H.; Yamakata, A.; Sakata, Y. Investigation on the highly active SrTiO₃ photocatalyst toward overall H₂O splitting by doping Na ion. *J. Catal.* **2020**, *390*, 81–89. [[CrossRef](#)]
63. Gholamrezaei, S.; Niasari, M.S.; Dadkhah, M.; Sarkhosh, B. New modified sol-gel method for preparation SrTiO₃ nanostructures and their application in dye-sensitized solar cells. *J. Mater. Sci. Mater. Electron.* **2015**, *27*, 118–125. [[CrossRef](#)]
64. Yoneyama, H.; Koizumi, M.; Tamura, H. Photolysis of Water on Illuminated Strontium Titanium Trioxide. *Bull. Chem. Soc. Jpn.* **1979**, *52*, 3449–3450. [[CrossRef](#)]
65. Zhu, L.; Gu, W.; Chen, J.; Liu, H.; Zhang, Y.; Wu, Q.; Zhang, Y.; Fu, Z.; Lu, Y. Improving the photocatalytic hydrogen production of SrTiO₃ by in situ loading ethylene glycol as a co-catalyst. *Inorg. Chem. Front.* **2020**, *7*, 4133–4141. [[CrossRef](#)]
66. Mai, X.T.; Bui, D.N.; Pham, V.K.; Hien, T.; Nguyen, L.; To, T.; Nguyen, L. Effect of CuO Loading on the Photocatalytic Activity of SrTiO₃ for Hydrogen Evolution. *Inorganics* **2022**, *10*, 130. [[CrossRef](#)]
67. Guo, M.; Liu, Q.; Wu, M.; Lv, T.; Jia, L. Novel reduced graphene oxide wrapped-SrTiO₃ flower-like nanostructure with Ti-C bond for free noble metal decomposition of formic acid to hydrogen. *Chem. Eng. J.* **2018**, *334*, 1886–1896. [[CrossRef](#)]
68. Zou, J.-P.; Zhang, L.-Z.; Luo, S.-L.; Leng, L.-H.; Luo, X.-B.; Zhang, M.-J.; Luo, Y.; Guo, G.-C. Preparation and photocatalytic activities of two new Zn-doped SrTiO₃ and BaTiO₃ photocatalysts for hydrogen production from water without cocatalysts loading. *Int. J. Hydrogen Energy* **2012**, *37*, 17068–17077. [[CrossRef](#)]
69. Zhou, D.; Zhai, P.; Hu, G.; Yang, J. Upconversion luminescence and enhanced photocatalytic hydrogen production for Er³⁺ doped SrTiO₃ nanoparticles. *Chem. Phys. Lett.* **2018**, *711*, 77–80. [[CrossRef](#)]

70. Zhou, M.; Chen, J.; Zhang, Y.; Jiang, M.; Xu, S.; Liang, Q.; Li, Z. Shape-controlled synthesis of golf-like, star-like, urchin-like and flower-like SrTiO₃ for highly efficient photocatalytic degradation and H₂ production. *J. Alloy. Compd.* **2019**, *817*, 152796. [[CrossRef](#)]
71. Jia, A.; Liang, X.; Su, Z.; Zhu, T.; Liu, S. Synthesis and the effect of calcination temperature on the physical–chemical properties and photocatalytic activities of Ni,La codoped SrTiO₃. *J. Hazard. Mater.* **2010**, *178*, 233–242. [[CrossRef](#)] [[PubMed](#)]
72. da Silva, L.F.; Lopes, O.F.; de Mendonça, V.R.; Carvalho, K.T.G.; Longo, E.; Ribeiro, C.; Mastelaro, V.R. An Understanding of the Photocatalytic Properties and Pollutant Degradation Mechanism of SrTiO₃ Nanoparticles. *Photochem. Photobiol.* **2016**, *92*, 371–378. [[CrossRef](#)] [[PubMed](#)]
73. Puangpetch, T.; Sreethawong, T.; Chavadej, S. Hydrogen production over metal-loaded mesoporous-assembled SrTiO₃ nanocrystal photocatalysts: Effects of metal type and loading. *Int. J. Hydrogen Energy* **2010**, *35*, 6531–6540. [[CrossRef](#)]
74. Sakata, Y.; Miyoshi, Y.; Maeda, T.; Ishikiriyama, K.; Yamazaki, Y.; Imamura, H.; Ham, Y.; Hisatomi, T.; Kubota, J.; Yamakata, A.; et al. Photocatalytic property of metal ion added SrTiO₃ to Overall H₂O splitting. *Appl. Catal. A Gen.* **2015**, *521*, 227–232. [[CrossRef](#)]
75. Takata, T.; Domen, K. Defect Engineering of Photocatalysts by Doping of Aliovalent Metal Cations for Efficient Water Splitting. *J. Phys. Chem. C* **2009**, *113*, 19386–19388. [[CrossRef](#)]
76. Gao, H.; Yang, H.; Wang, S. Hydrothermal synthesis, growth mechanism, optical properties and photocatalytic activity of cubic SrTiO₃ particles for the degradation of cationic and anionic dyes. *Optik* **2018**, *175*, 237–249. [[CrossRef](#)]
77. Trawiński, J.; Skibiński, R. Multivariate comparison of photocatalytic properties of thirteen nanostructured metal oxides for water purification. *J. Environ. Sci. Health Part A* **2019**, *54*, 851–864. [[CrossRef](#)]
78. Galloni, M.G.; Cerrato, G.; Giordana, A.; Falletta, E.; Bianchi, C.L. Sustainable Solar Light Photodegradation of Diclofenac by Nano- and Micro-Sized SrTiO₃. *Catalysts* **2022**, *12*, 804. [[CrossRef](#)]
79. Song, Y.; Hao, X.; Dai, W.; Zhao, J. Aqueous Synthesis and Photocatalytic Performance of Bi₅O₇I Microflowers. *Nano* **2019**, *14*, 1950050. [[CrossRef](#)]
80. Wu, G.; Xiao, L.; Gu, W.; Shi, W.; Jiang, D.; Liu, C. Fabrication and excellent visible-light-driven photodegradation activity for antibiotics of SrTiO₃ nanocube coated CdS microsphere heterojunctions. *RSC Adv.* **2016**, *6*, 19878–19886. [[CrossRef](#)]
81. Nunes, M.J.; Lopes, A.; Pacheco, M.J.; Ciriaco, L. Visible-Light-Driven AO7 Photocatalytic Degradation and Toxicity Removal at Bi-Doped SrTiO₃. *Materials* **2022**, *15*, 2465. [[CrossRef](#)] [[PubMed](#)]